

One-Step Preparation of Porous Silica Spheres from Sodium Silicate Using Triblock Copolymer Templating

Katsunori Kosuge,* Nobuyuki Kikukawa, and Makoto Takemori

Adsorption and Decomposition Technology Research Group, Research Institute for Environmental Management Technology, National Institute of Advanced Industrial Science and Technology, 16-1 Onogawa, Tsukuba-shi, Ibaraki, 305-8569 Japan

Received February 3, 2004. Revised Manuscript Received July 5, 2004

Mesoporous and microporous monodispersed silica spheres have been prepared using a simple one-step synthetic procedure from an aqueous reaction mixture consisting of a commercial sodium silicate solution, various Pluronic triblock copolymers, and HCl or HNO₃. The formation of porous silica spheres 130–225 μm in diameter was observed over a moderately wide range of reaction conditions. The pore structures of the resultant spheres lacked any long-range order, although they did exhibit outer textural uniformity. We concluded that the well-defined spherical morphology and pore sizes were the result of a combined effect of the EO/(EO + PO) block ratio and molecular weight of the Pluronics and the counteranions of the acid source.

Introduction

Over 10 years after the discovery of mesoporous materials,¹ the synthesis of hierarchically ordered structures on different length scales has attracted a great deal of interest from both a fundamental and practical viewpoint.² Since the first report of the synthesis of M41S-type mesoporous silica spheres through a modification of Stöber's procedure,³ many kinds of mesoporous silica spheres have been synthesized through various assembly pathways,^{4,5} including S⁺I⁻, S⁺X⁻I⁺, and an evaporation-induced self-assembly process⁶ using cationic surfactants. In addition, various hollow mesoporous silica spheres have also been produced by the controlled hydrolysis of silicon alkoxides in stabilized emulsions of biphasic systems.⁷ The [N⁰I⁰]⁸ and [S⁰H⁺][X⁻I⁺]⁹ assembly pathways using poly-

(ethylene oxide) (PEO) nonionic surfactant templating have also led to the formation of mesoporous spheres.

It was first believed that uniform mesoporous silica spheres would be produced easily, but most of the spheres produced have not been in the form of uniform monodispersed particles. Mesoporous spheres on the order of 100 μm are desirable for industrial applications such as catalytic, separation, and adsorption processes because they can be easily packed into existing reactors, columns, or fixed and fluidized beds in various reaction systems. However, the diameter of almost all conventional products to this point is less than ca. 10 μm excluding a few examples.^{4,10} In addition, most of the conventional products required a reaction time of 1–3 days, additional additives such as surfactants and solvents, and hydrothermal treatment in their preparation. In all of these cases described above, silicon alkoxide, an expensive organic silica precursor, was used.

Since the first report by Sierra and Guth¹¹ of a synthesis using low-cost sodium silicate in place of costly silicon alkoxides as a silica source with a nonionic poly-(ethylene oxide) surfactant, some research groups have prepared thermally stable mesoporous silica products using sodium silicate solutions by block copolymer templating.^{12–14} However, very few studies have ad-

* Corresponding author. Telephone: +81-29-861-8179. Fax: +81-29-861-8459. E-mail: k.kosuge@aist.go.jp.

(1) (a) Beck, J. S.; Vartuli, J. C.; Roth, W. J.; Leonowicz, M. E.; Kresge, C. T.; Schmitt, K. D.; Chu, C. T.-W.; Olson, D. H.; Sheppard, E. W.; McCullen, B.; Higgins, J. B.; Schlenker, J. L. *J. Am. Chem. Soc.* **1992**, *114*, 10834. (b) Inagaki, S.; Fukushima, Y.; Kuroda, K. *Chem. Commun.* **1993**, 680.

(2) (a) Ciesla, U.; Schüth, F. *Microporous Mesoporous Mater.* **1999**, *27*, 131. (b) Stein, A. *Adv. Mater.* **2003**, *15*, 763.

(3) Grün, M.; Lauer, I.; Unger, K. K. *Adv. Mater.* **1997**, *9*, 254.

(4) Huo, Q.; Feng, J.; Schüth, F.; Stucky, G. D. *Chem. Mater.* **1997**, *9*, 14.

(5) (a) Yang, H.; Vovk, G.; Coombs, N.; Sokolov, I.; Ozin, G. A. *J. Mater. Chem.* **1998**, *8*, 743. (b) Gallis, K. W.; Araujo, J. T.; Duff, K. J.; Moore, J. G.; Landry, C. C. *Adv. Mater.* **1999**, *11*, 1452. (c) Unger, K. K.; Kumar, D.; Grün, M.; Büchel, G.; Lüdtkke, S.; Adam, T.; Schumacher, K.; Renker, S. *J. Chromatogr. A* **2000**, *892*, 47. (d) Nooney, R. I.; Thirunavukkarasu, D.; Chen, Y.; Josephs, R.; Ostafin, A. E. *Chem. Mater.* **2002**, *14*, 4721. (e) Ma, Y.; Qi, L.; Ma, J.; Wu, Y.; Liu, O.; Cheng, H. *Colloids and Surfaces A* **2003**, *229*, 1. (f) Yano, K.; Fukushima, Y. *J. Mater. Chem.* **2003**, *13*, 2577.

(6) (a) Lu, Y.; Fan, H.; Stump, A.; Ward, T. L.; Rieker, T.; Brinker, C. J. *Nature* **1999**, *398*, 223. (b) Brinker, C. J.; Lu, Y.; Sellinger, A.; Fan, H. *Adv. Mater.* **1999**, *11*, 579. (c) Rama Rao, G. V.; López, G. P.; Bravo, J.; Pham, H.; Datye, A. K.; Xu, H.; Ward, T. L. *Adv. Mater.* **2002**, *14*, 1301.

(7) (a) Schacht, S.; Huo, Q.; Voigt-Martin, I. G.; Stucky, G. D.; Schüth, F. *Science*, **1996**, *273*, 768. (b) Fowler, C. E.; Khushalani, D.; Mann, S. *Chem. Commun.* **2001**, 2028. (c) Li, W.; Sha, X.; Dong, W.; Wang, Z. *Chem. Commun.* **2002**, 2434.

(8) Boissière, C.; van der Lee, A.; El Mansouri, A.; Larbot, A.; Prouzet, E. *Chem. Commun.* **1999**, 2047.

(9) Zhao, D.; Sun, J.; Li, Q.; Stucky, G. D. *Chem. Mater.* **2000**, *12*, 275.

(10) Kosuge, K.; Murakami, T.; Kikukawa, N.; Takemori, M. *Chem. Mater.* **2003**, *15*, 3184.

(11) Sierra, L.; Guth, J.-L. *Microporous Mesoporous Mater.* **1999**, *28*, 243.

(12) Kim, S. S.; Pauly, T. R.; Pinnavaia, T. J. *Chem. Commun.* **2000**, 835.

dressed the possibility of forming well-defined macroscopic morphological products, such as silica spheres, using sodium silicate and PEO-based surfactant templating.^{15,16} Examples of spherical silicas include MSU-X with a diameter of ca. 10 μm prepared by a two-step synthesis¹⁵ and hollow silica spheres of <1 μm in size,¹⁶ both of which were synthesized using additives.

It is important in the synthesis of porous spherical materials that the products are entirely uniform in macroscopic shape and have a controllable pore size and particle size. The present work describes a simple one-step synthetic approach in forming porous silica spheres over 100 μm in diameter with a high monodispersity. The spheres are prepared using a combination of an inorganic silica precursor and various Pluronic under acidic conditions without additional additives. It was observed, for the first time, that the counteranions of the acid source directly affect the outer shape and inner structure of the products, in addition to the hydrophobicity and molecular weight of the polymer surfactants.

Experimental Section

Materials Synthesis. Mesoporous silica spheres were synthesized using various triblock copolymers, commercially supplied as Pluronics [poly(ethylene oxide)-poly(propylene oxide)-poly(ethylene oxide); $\text{EO}_m\text{PO}_n\text{EO}_m$], as templates and a sodium silicate solution (SiO_2 23.6%, Na_2O 7.59%) as a silicate framework source under acidic conditions. All commercial chemicals were used without purification. Between 0.75 and 2 g of triblock copolymer was dissolved in 30–80 g of aqueous HCl or HNO_3 at 30 $^\circ\text{C}$. This solution was then quickly added to a mixture of 5.2 g of the sodium silicate solution and 15 g of deionized water at 30 $^\circ\text{C}$ with stirring. The reaction mixture was stirred continuously at 600 rpm for 2 h using a Highflex Disperser (HG92; SMT Co., Ltd.). The stirring speed was changed over the range from 400 to 1000 rpm for two Pluronic species (P104 and F88) to investigate the effect of stirring speed on the resultant particle size and porous parameters. Particle formation of monodispersed spheres proceeded gradually from an initial transparent solution through a turbid suspension to a clear solution of spherical particles. The product yields were perfect on the basis of silica recovery for reaction times of 2 h. The solid product was filtered and washed repeatedly with warm deionized water, dried, and then calcined at 600 $^\circ\text{C}$ for 1 h in air.

It is well-known that various parameters, such as reaction temperature, the surfactant/silica ratio, and the anions present in the reaction, can greatly influence the final mesostructure and morphology of the products. Although coexisting inorganic salts also affect both characteristics,^{17,18} the amount of inorganic salts present was almost constant at $\text{Na}_2\text{O}/\text{SiO}_2 = 0.312$ in our reaction system. The optimum one-step synthetic conditions for the formation of uniform monodispersed spheres were investigated at various reaction mixtures of $\text{SiO}_2/\text{acid}/\text{H}_2\text{O}$ [1:(2.0–10):(100–220)] for each Pluronic without any additional additives such as surfactants or solvents. The

Pluronics used here were referred to as group I (P104, P105, and P85), group II (F108, F88, and F68), group III (F127), and others are denoted as group IV (L121, L64, P65, P123, P103, and P84). This classification was determined on the basis of the experimental results regarding the role of the counterions plus the various listed Pluronics in the formation of the products.

Characterization. The powder X-ray diffraction (XRD) patterns were obtained with a small-angle X-ray scattering NANO-Viewer (Rigaku Corp.) equipped with a rotating anode using Cu K α radiation at 45 kV and 60 mA. Scanning electron microscopy (SEM) images were obtained with a JEOL5300, and transmission electron microscopy (TEM) images were obtained with a JEOL 2000FX. The particle size distribution was measured using a Coulter Multisizer III and evaluated by a volume concentration. The N_2 sorption isotherms were obtained at -196 $^\circ\text{C}$ on a BELSORP 28 under continuous adsorption conditions. Prior to measurement, samples were heated at 200 $^\circ\text{C}$ for 2 h and then outgassed to 10^{-3} Torr at room temperature. BET analysis was used to determine the total specific surface area (S_{BET}). The total pore volume (V_{total}) and micropore volume (V_{micro}) of the products were calculated using a t -plot analysis.¹⁹ Mesopore size distributions were calculated using the BJH method.

Results and Discussion

Effects of the Counterion Species. It is well-known that differences in the nucleation and growth rates are important factors for monodispersed particle formation, with a higher degree of separation between the nucleation and growth processes leading to more monodispersed particles.²⁰ $[\text{S}^0\text{H}^+][\text{X}^-]$ assemblies promote the formation of mesostructured primary particles from which growth is inferred to yield monodispersed hard spheres under our reaction conditions. Table 1 shows the reactant molar ratios with respect to SiO_2 , including the PO molecular weight, PO amount, and $\text{EO}/(\text{EO} + \text{PO})$ ratio of the surfactants. The reaction ratios shown in Table 1 are the optimum values for the preparation of monodispersed particles specific for each Pluronic. Hereafter, sample names denoted as S1, S2, etc. will be used in describing the various reactions.

In the acid synthesis pathway of $\text{S}^+\text{X}^-\text{I}^+$, the macroscopic morphology of MCM-41 silicas was selectively controlled by using HNO_3 and HCl.²¹ The interface interactions of the $[\text{S}^0\text{H}^+][\text{X}^-]$ assembly, mediated by the counteranion X^- , influence how the final products organize themselves on different length scales.^{18b,22} In our work, NO_3^- mediation resulted in the formation of monodispersed spheres with a diameter of over 100 μm in Pluronic group I (P104, P105, and P85), group II (F108, F88, and F68), and group III (F127). The SEM images of the corresponding samples from the above groups (S1, S4, S5, S2, S3, S7, and S6) are shown in Figure 1. Samples S4, S5, S6, and S7 clearly exhibited a lower level of monodispersity and/or a relatively broad particle size distribution based on the SEM images.

In contrast, Cl^- mediation resulted in the formation of monodispersed spheres (S8 and S9) only for Pluronic

(13) Kim, J. M.; Stucky, G. D. *Chem. Commun.* **2000**, 1159.

(14) (a) Kim, S. S.; Pauly, T. R.; Pinnavaia, T. J. *Chem. Commun.* **2000**, 1661. (b) Kim, S. S.; Karkamkar, A.; Pinnavaia, T. J.; Kruk, M.; Jaroniec, M. *J. Phys. Chem. B* **2001**, *105*, 7663. (c) Joo, S. H.; Ryoo, R.; Kruk, M.; Jaroniec, M. *J. Phys. Chem. B* **2002**, *106*, 4640.

(15) Boissiere, C.; Larbot, A.; Prouzet, E. *Chem. Mater.* **2000**, *12*, 1937.

(16) Sun, Q.; Kooyman, P. J.; Grossmann, J. G.; Bomans, P. H. H.; Frederik, P. M.; Magusin, P. C. M. M.; Beelen, T. P. M.; van Santen, R. A.; Sommerdijk, N. A. J. M. *Adv. Mater.* **2003**, *15*, 1097.

(17) Leontidis, E. *Curr. Opin. Colloid Interface Sci.* **2002**, *7*, 81.

(18) (a) Yu, C.; Tian, B.; Fan, J.; Stucky, G. D.; Zhao, D. *Chem. Commun.* **2001**, 2726. (b) Yu, C.; Tian, B.; Fan, J.; Stucky, G. D.; Zhao, D. *J. Am. Chem. Soc.* **2002**, *124*, 4556. (c) Flodström, K.; Alfredsson, V.; Källrot, N. *J. Am. Chem. Soc.* **2003**, *125*, 4402.

(19) Gregg, S. G.; Sing, K. S. W. *Adsorption Surface Area and Porosity*, 2nd ed.; Academic Press: New York, 1982.

(20) (a) Sugimoto, T. *Adv. Colloid Interface Sci.* **1987**, *28*, 65. (b) Ocaña, M.; Rodríguez-Clemente, R.; Serna, C. J. *Adv. Mater.* **1995**, *7*, 212.

(21) (a) Lin, H. P.; Kao, C. P.; Mou, C. Y.; Liu, S. B. *J. Phys. Chem. B* **2000**, *104*, 7885. (b) Lin, H. P.; Mou, C. Y. *Acc. Chem. Res.* **2002**, *35*, 927.

(22) Bagshaw, S. A. *J. Mater. Chem.* **2001**, *11*, 831.

Table 1. Synthetic Conditions and Porous Properties of Representative Spheres

sample name	pluronic surfactant			reactant composition ^d			S_{BET} (m ² /g)	V_{total} (mL/g)	V_{micro} (mL/g)	D_{pore} (nm)	d spacing (nm)	R (mm)
	species (M_{av}) ^a	M_{PO} ^b	R_{EO} ^c	surfactant	acid	H ₂ O						
S1	P104 (5900)	3540	0.4	0.017	5.68 (HNO ₃)	196	910	0.61	0.15	4.42	8.14	175
S2	F108 (14600)	2920	0.8	0.005	3.72 (HNO ₃)	146	841	0.41	0.24	3.80	10.10	129
S3	F88 (11400)	2280	0.8	0.006	3.73 (HNO ₃)	146	802	0.37	—	—	8.75	131
S4	P105 (6500)	3250	0.5	0.008	5.56 (HNO ₃)	193	860	0.51	0.15	3.95	—	195
S5	P85 (4600)	2300	0.5	0.021	5.61 (HNO ₃)	194	767	0.37	—	—	—	—
S6	F127 (12600)	3780	0.7	0.004	5.63 (HNO ₃)	195	668	0.37	0.17	4.55	10.39	133
S7	F68 (8400)	1680	0.8	0.006	5.65 (HNO ₃)	195	797	0.33	—	—	—	—
S8	F108 (14600)	2920	0.8	0.005	3.75 (HCl)	148	759	0.37	0.21	3.80	—	151
S9	F88 (11400)	2280	0.8	0.006	3.86 (HCl)	152	781	0.37	—	—	—	171
S10	P104 (5900)	3540	0.4	0.017	5.77 (HCl)	198	909	0.66	0.11	4.37	—	—
S11	P123 (5800)	4060	0.3	0.017	5.61 (HNO ₃)	250	826	0.57	0.13	4.58	7.48	—
S12	P104 (5900)	3540	0.4	0.008	5.66 (HNO ₃)	147	925	0.53	0.16	3.90	7.75	225
S13	mix 1 ^e	—	—	0.013	5.71 (HNO ₃)	196	916	0.54	0.17	4.15	9.50	138
S14	F88 (11400)	2280	0.8	0.006	5.26 (HCl)	202	705	0.35	—	—	8.58	165
S15	F88 (11400)	2280	0.8	0.006	4.40 (HCl)	203	791	0.43	0.17	3.70	8.49	—
S16 ^f	P104 (5900)	3540	0.4	0.017	5.68 (HNO ₃)	196	851	0.60	0.15	4.51	—	145
S17 ^f	F88 (11400)	2280	0.8	0.006	3.73 (HNO ₃)	146	813	0.38	—	—	—	106

^a M_{av} , Molecular weight. ^b M_{PO} , PO weight in one molecule. ^c R_{EO} , EO weight ratio in one molecule. ^d Molar ratio for SiO₂. ^e Mixed Pluronics of P104 and F127 with 0.78:0.22. ^f Stirring speed is 700 rpm. S_{BET} , BET surface area; V_{total} , V_{micro} , primary total pore and microporous volume evaluated by the t -plot method, respectively; D_{pore} , BJH mesopore diameter calculated from the adsorption branch; R , mean particle diameter.

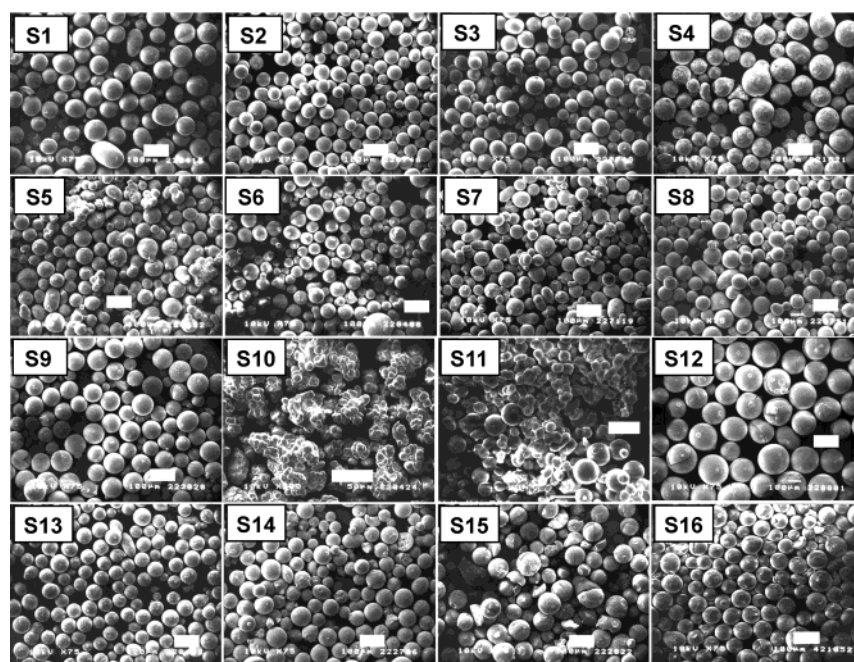


Figure 1. SEM micrographs of various samples of which the names are denoted in Table 1. Each scale bar is equal to 200 μm , except for S10 and S11, in which the scale bar is 50 and 10 μm , respectively.

group II, in which the particle-shape quality was equivalent to the samples (S2 and S3) obtained by NO₃[−] mediation. However, in the case of Pluronic group I and group III, Cl[−] mediation resulted in the formation of aggregates composed of smaller spheres, as shown in Figure 1 (S10).

The formation of spherical particles occurred with various Pluronics in the presence of nitrate ion, presumably because NO₃[−] is more hydrophilic than Cl[−].^{17,21} This would lead to much stronger binding between the nitrate ions and EO blocks, and the subsequent quick progression to silica condensation in our reaction solution consisting of a sodium silicate and Pluronic triblock copolymer.²³ On the other hand, Cl[−] mediation might

have assisted in the formation of the silica spheres for Pluronic group II because of the slow-down of silica condensation caused by the presence of additional EO. Larger EO amounts led to a more hydrophilic environment, which may compensate for the lower hydrophilicity of Cl[−] relative to NO₃[−]. For groups I and III, this compensatory affect was not present due to lower EO amounts, and as a result, these reactions did not yield monodisperse spheres.

Furthermore, monodispersed spheres were not obtained for Pluronic group IV (L121, L64, P65, P123, P103, P84) in the presence of Cl[−] or NO₃[−]. Only aggregated or fragmented particles were formed for this group. A past study reported that the use of a cosurfactant together with P123 yielded a spherical silica with a diameter < 5 μm in the presence of TEOS.⁹ In our simple one-step procedure, P123, a very attractive

(23) Kosuge, K.; Sato, T.; Kikukawa, N.; Takemori, M. *Chem. Mater.* **2004**, *16*, 899.

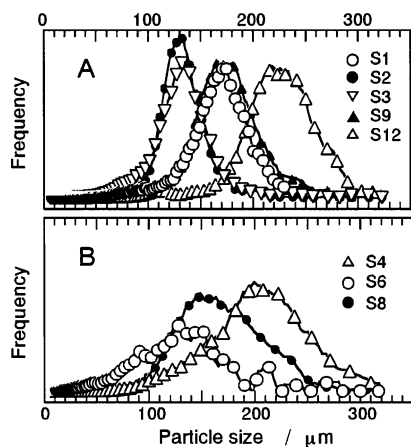


Figure 2. Particle size distributions of representative samples of which the names are denoted in Table 1.

Pluronic, never yielded monodispersed spheres at any of the experimental reaction temperatures, although NO_3^- mediation did lead to the formation of agglomerated particles comprised of nearly spherical constituents, as shown in Figure 1 (S11). These results are consistent with the fact that P123 exhibits a very strong hydrophobicity that leads to a stronger tendency to form elongated cylindrical silicated-surfactant micelles.²⁴ However, NO_3^- mediation should lead to rapid silica condensation, which should result in the formation of nearly spherical particles even in the case of P123.

Control of Particle Size. Figure 2 shows the representative particle size distribution curves analyzed by the volume concentration. The mean particle sizes of the products are listed in Table 1. The particle size distributions for the well-defined spheres seem to become a little sharper with decreasing particle size, as shown in Figure 2A. However, the samples of S4 and S6 have a relatively broad particle size distribution, which is consistent with SEM observation in Figure 1. Further, SEM observation revealed that the order of the spherical shape and the uniformity of the particle size distribution were affected by the stirring rate. Monodispersed spheres with good quality were obtained in the range of 500–700 rpm. A spherical morphology was not observed at speeds over 800 rpm.

It should be noted that the particle size of the products was controllable by changing the reactant ratios, by slightly increasing the stirring speed, or by using a mixture of Pluronics, as shown in Figure 1. Relatively large (225 μm , S12), medium (175 μm , S1), and small (145 μm , S16; 138 μm , S13) spheres were obtained using P104, indicating that mesoporous spheres with different particle sizes can be prepared. This observation is also supported by comparing the spheres formed when P88 and F108 were used (S2, S3, S8, S9, and S17). In these reactions, Cl^- mediation resulted in a particle size of over 150 μm (S8 and S9) compared with a particle size of ca. 130 μm from NO_3^- mediation (S2 and S3).

Sorption Properties. Figure 3 shows N_2 sorption isotherms for the silica spheres of S1–S15 shown in Figure 1. Table 1 summarizes the porous properties of

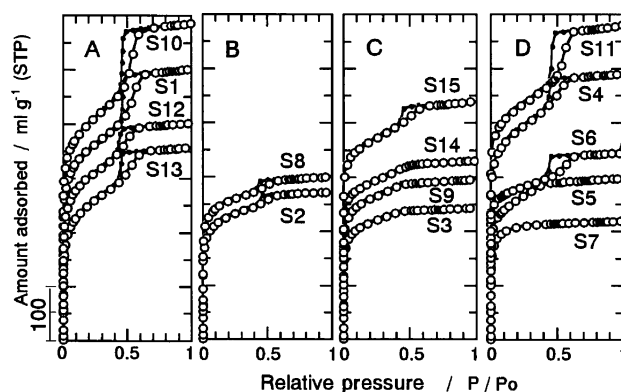


Figure 3. Nitrogen sorption isotherms for the samples listed in Table 1. Open symbols, adsorption; closed symbols, desorption. Isotherms are offset by 50 mL/g for clarity.

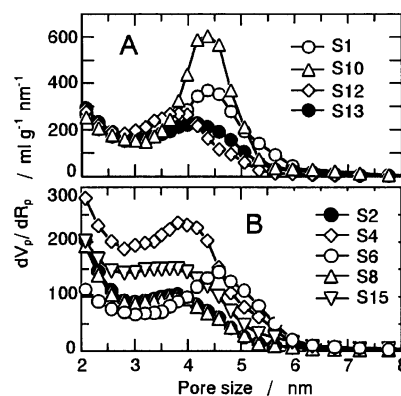


Figure 4. Pore size distributions of mesoporous samples obtained using P104 (A) and another Pluronics (B).

these products. Under our reaction conditions, the stirring speed had only a small effect on the porous parameters so long as the monodispersity of the spheres was maintained (S1 and S16, and S3 and S17). Hence, the primary mesophases, from which assembly would lead to spheres, would have very similar structures, irrespective of the stirring speed. Figure 3 shows the difference in mesoporosity resulting from a difference in the counteranion. Sample S10, obtained using HCl with P104, exhibited a higher quality of mesoporosity than S1, prepared using HNO_3 . However, S10 did not result in monodispersed spheres (Figure 1). Furthermore, in the case of F88, the Cl^- mediation also caused a slight increase in the degree of mesoporosity while a spherical morphology was maintained (S14, Table 1 and Figure 3C). However, a lower concentration did result in the fragmentation of spheres along with an increase in particle size (S15). These data demonstrate the effects of the counteranion on pore structure. It should be noted that the formation of monodispersed spheres would have to be sacrificed for a more highly ordered mesostructural phase based on our data.

Figure 4 shows the pore size distribution of the mesoporous products. The pore size decreased with a decrease in the PO amount and an increase in the EO/(EO + PO) ratio, as summarized in Table 1. Although all reactions with PO amounts below 3000 formed predominantly microporous products, we were unable to calculate a BJH pore size distribution curves for samples S3, S5, S7, and S9. S14 had too broad a distribution to evaluate the mean pore size (not shown).

(24) (a) Wanka, G.; Hoffmann, H.; Ulbricht, W. *Macromolecules* **1994**, *27*, 4145. (b) Alexandridis, P.; Hatton, T. A. *Colloids Surf. A* **1995**, *96*, 1. (c) Mortensen, K. *Polym. Adv. Technol.* **2001**, *12*, 2.

Furthermore, from t -plots for N_2 adsorption isotherms, for which the intercept of the extrapolated linear region corresponds to micropore volume,^{19,25} such volume would increase concomitant with the increasing of EO/(EO + PO) ratio used in Pluronics and then would be slightly larger for NO_3^- mediation than for Cl^- mediation for the same surfactant, as shown in Table 1. It is well-known that hydrophilic EO blocks lead to additional microporosity as a consequence of molecular templating of the EO chains.^{25,26} This would explain why the samples obtained using more hydrophilic Pluronics have a larger micropore volume (Table 1). Furthermore, it has been reported that the aggregation number and core size in micelles decreases by increasing the EO amount in the Pluronics.²⁴ This presumably results in the formation of predominantly microporous materials of which the pore sizes formed by both the PO and EO blocks might be nearly identical. These results would indicate a more intimate interlinkage of the longer EO blocks with the silica species during solidification.

Pore Structures. Pluronic copolymers form spherical micelles comprised of a core dominated by hydrophobic PO blocks surrounded by a corona of hydrated EO blocks. In addition, their intermicellar interactions result in various crystalline structures on the mesoscopic length scale.²⁴ Previous work^{27,28} on the synthesis of mesoporous silica structures using triblock copolymers indicated that the EO/(EO + PO) ratio and polymer molecular weight have a large effect on the mesophase structures of mesoporous silica products in aqueous acidic systems. Ratios of EO/(EO + PO) ≤ 0.6 (in this work, Pluronic groups I and IV) and higher ratios of >0.6 (Pluronics groups II and III) were found to favor the formation of hexagonal and cubic mesophase structures, respectively. However, the small-angle X-ray diffraction patterns of the spherical samples in this study showed one peak at a d spacing of ca. 7.7–10.4 nm. Figure 5 depicts representative XRD patterns. The patterns of S1, S2, and S6 are characteristic of mesoporous materials with a pore structure that lacks long-range order.²⁹ The intensity of the d_{100} reflection for S3 is extremely low, indicating that the micropore dominant products seem to form an amorphous phase with less ordered porous structures. The pore structures expected from the XRD patterns should be apparent with the high-resolution TEM images (Figure 6). Figure 6 indicates that S6 has a relatively well-ordered pore structure in comparison with the others. S1 has a typical wormhole-like pore structure, whereas an amorphous phase-like texture can be observed for S2 as a result of the smaller pore sizes. In addition, an amorphous

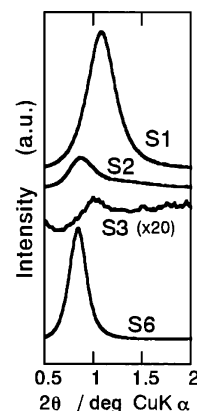


Figure 5. Small angle XRD patterns of representative samples of S1, S2, S3, and S6.

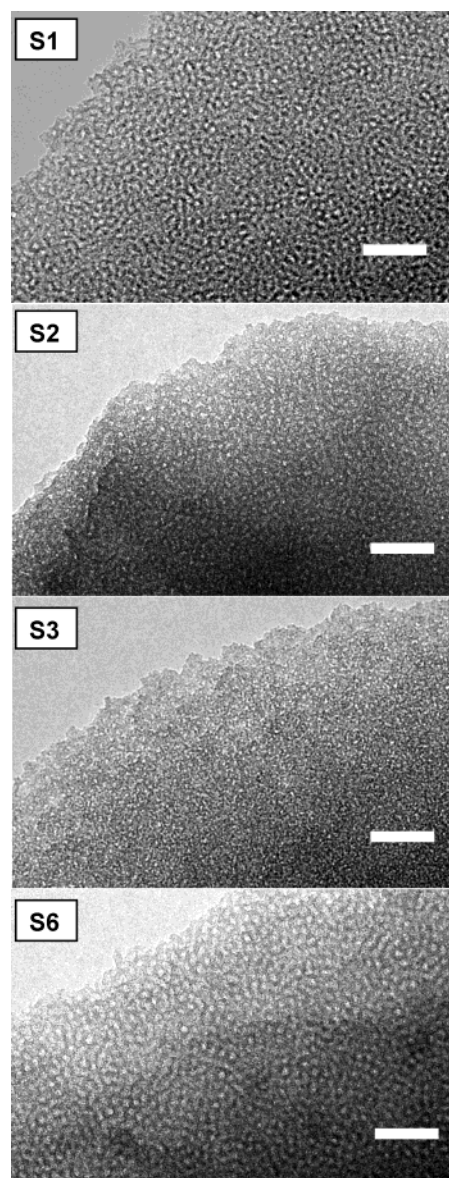


Figure 6. TEM micrographs of S1, S2, S3, and S6. Scale bars show 50 nm.

texture can also be seen for S3. The d spacings in the XRD patterns and the pore sizes evaluated from the N_2 isotherms for each spherical product would indicate that products prepared using more hydrophilic Pluronics have thicker pore walls.

(25) (a) Miyazawa, K.; Inagaki, S. *Chem. Commun.* **2000**, 2121. (b) Galarneau, A.; Cambon, H.; Renzo, F. D.; Fajula, F. *Langmuir* **2001**, *17*, 8328.

(26) (a) Kruk, M.; Jaroniec, M.; Ko, C. H.; Ryoo, R. *Chem. Mater.* **2000**, *12*, 1961. (b) Clere, M. I.; Davidson, P.; Davidson, A. *J. Am. Chem. Soc.* **2000**, *122*, 11925.

(27) (a) Zhao, D.; Feng, J.; Huo, Q.; Melosh, N.; Fredrickson, G. H.; Chmelka, B. F.; Stucky, G. D. *Science* **1998**, *279*, 548. (b) Zhao, D.; Huo, Q.; Feng, J.; Chmelka, B. F.; Stucky, G. D. *J. Am. Chem. Soc.* **1998**, *120*, 6024.

(28) (a) Kipkemboi, P.; Fogden, A.; Alfredsson, V.; Flodström, K. *Langmuir* **2001**, *17*, 5398. (b) Flodström, K.; Alfredsson, V. *Microporous Mesoporous Mater.* **2003**, *59*, 167.

(29) (a) Tanev, P. T.; Chibwe, M.; Pinnavaia, T. J. *Nature* **1994**, *368*, 321. (b) Bagshaw, S. A.; Prouzet, E.; Pinnavaia, T. J. *Science* **1995**, *269*, 1242.

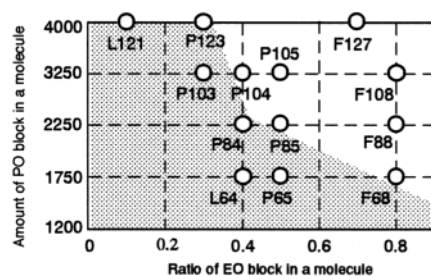


Figure 7. The formation of monodispersed silica spheres is shown in the bright region. Circles indicate the Pluronics used in this paper. The templating with Pluronic group I (P104, P105, and P85), and group III (F127) caused the formation of spheres only when HNO_3 was used, and group II (F108, F88, and F68) yielded spheres when either HNO_3 or HCl was used. However, only aggregated or fragmented particles were formed for group IV (L121, L64, P65, P123, P103, P84) using either acid.

Our experimental results indicate that monodispersed spheres formed in the region of $\text{EO}/(\text{EO} + \text{PO})$ ratio > 0.3 with a PO amount over 1700 and a total molecular weight over 4600 in our one-step procedure. Figure 7 shows the formation region of monodispersed silica spheres. Moreover, it was found that mesoporous spheres with micropores were clearly formed with a PO molec-

ular weight above 3000, while predominantly microporous spheres tend to be produced below 3000.

Conclusions

The practical uses of mesoporous silica spheres have created a desire for more cost-effective and "environmentally friendly" approaches for their synthesis and for better-defined macroscopic morphologies of the products. We carried out a one-step selective preparation of monodispersed mesoporous and micropore dominant spheres with a diameter of over $100\ \mu\text{m}$ using a commercial sodium silicate solution and various Pluronics. Both kinds of spheres were formed at $\text{EO}/(\text{EO} + \text{PO})$ ratio > 0.3 with a molecular weight over 4600. Predominantly microporous spheres were obtained with a PO molecular weight below 3000. Formation of monodispersed spheres would be sacrificed for a higher order of mesostructural phases; hence, the resulting spheres would have pore structures lacking long-range order with relatively uniform pore sizes. The particle size was controllable within $130\text{--}225\ \mu\text{m}$ by changing the reaction composition, by altering the stirring speed, and by mixing different Pluronics.

CM0400177